Fine-scale vertical structure of sound scattering layers over an east border upwelling system and its relationship to pelagic habitat characteristics

Ndague DIOGOUL[1,6,*], Patrice BREHMER[2,3,6], Yannick PERROT[3], Maik TIEDEMANN[4], Abou THIAM[1], Salaheddine EL AYOUBI[5], Anne MOUGET[3], Chloé MIGAYROU[3], Oumar SADIO[2] and Abdoulaye SARRÉ[6]

[1] University Cheikh Anta Diop UCAD, Institute of Environmental Science (ISE), BP 5005 Dakar, Senegal

[2] IRD, Univ Brest, CNRS, Ifremer, LEMAR, Campus UCAD-IRD de Hann, Dakar, Senegal

[3] IRD, Univ Brest, CNRS, Ifremer, LEMAR, DR Ouest, Plouzané, France

[4] Institute of Marine Research IMR, Pelagic Fish, PO Box 1870 Nordnes, 5817 Bergen, Norway

[5] Institut National de Recherche Halieutique INRH, Agadir, Morocco

[6] Institut Sénégalais de Recherches agricoles ISRA, Centre de Recherches Océanographiques de Dakar-Thiaroye (CRODT), BP 2221 Dakar, Senegal

*Corresponding author: diogoulndague@yahoo.fr

Abstract

Understanding the relationship between sound scattering layers 'SSLs' and pelagic habitat characteristics is a substantial step to apprehend ecosystem dynamics. SSLs are detected on echosounders representing aggregated marine pelagic organisms. In this study, SSL characteristics of zooplankton and micronekton were identified during an upwelling event in two contrasting areas of the Senegalese continental shelf. Here a cold upwelling influenced inshore area was sharply separated by a strong thermal boundary from a deeper warmer stratified offshore area. Mean SSL thickness and SSL vertical depth increased with the shelf depth. The thickest and deepest SSLs were observed in the offshore part of the shelf. Hence, zooplankton and micronekton seem to occur more frequently in stratified water conditions rather than in fresh upwelled water. Diel vertical and horizontal migration of SSLs were observed in the study area. Diel period and physico-chemical water characteristics influenced SSL depth and SSL thickness. Although chlorophyll-*a* concentration insignificantly affected SSL characteristics, the peak of chlorophyll-*a* was always located above or in the middle of the

SSLs, regularly matching with the peak of SSL biomass. Such observations indicate trophic relationships, suggesting SSLs being mainly composed of phytoplanktivorous zooplankton and micronekton. Despite local hypoxia, below 30 m depth, distribution patterns of SSLs indicate no vertical migration boundary. The results increase the understanding of mid-trophic species spatial organisation, migration patterns of zooplankton and micronekton as well as will improve dispersal models for organisms in upwelling regions.

Keywords: pelagic organism, micronekton, diel vertical migration (DVM), hypoxia, Senegal, West Africa.

1 Introduction

Aggregations of marine pelagic organisms in ocean water can be observed acoustically as sound-scattering layers (SSLs) (Evans and Hopkins, 1981; Cascão et al., 2017). The SSLs represents a concentrated layer of marine organisms such as zooplankton aggregates and nekton that occur at specific depths (Benoit-Bird and Au, 2004; McManus et al., 2008). Nevertheless the "SSL" is not a biological classification, and animals making up SSLs include various species, with correspondingly different biological, physiological, and ecological needs. The SSLs are dynamic, active, and have a particular behavior as a function of their community structure causing changes in their vertical distribution, size, and shape over time and space (Gómez-Gutiérrez et al., 1999). Zooplanktonic and micronektonic components are fundamental to ecosystem functioning, particularly in productive upwelling areas (*e.g.*, off the south coast of Senegal).

Zooplanktonic and micronektonic provide the main trophic link between primary producers and and higher trophic levels. A large amount of energy passes through zooplankton and micronekton (Steele et al., 2007). Knowledge of the vertical structure of SSLs allows to understand their role in ecosystems, information that can be used to monitor major environmental change and variability. Most zooplankton and micronektonic taxa undergo diel vertical migration (DVM), meaning that they reside in deep waters during the day and migrate toward the surface at night to feed (Bianchi et al., 2013; Lehodey et al., 2015). DVM behaviors are influenced by environmental cues (*e.g.*, light, nutrients, and temperature) and predator-prey interactions (Clark and Levy, 1988; Lampert, 1989). Thus, DVMs represent an essential biological process in the ocean, one that also regulates the biological carbon pump (Hidaka et al., 2001). Zooplankton and micronekton are also known to undergo diel horizontal migration

(DHM), moving them to within 1 km of the shoreline each night into waters shallower (Benoit-Bird et al., 2001). DHM, like DVM, which often occur concurrently, help organisms find food and avoid predators (White, 1998).

The distribution of SSLs is influenced by a variety of environmental factors (Aoki and Inagaki, 1992; Baussant et al., 1992; Dekshenieks et al., 2001; Marchal et al., 1993). Changes in the structure and density of SSLs are associated with frontal zones (Aoki and Inagaki, 1992; Baussant et al., 1992; Boersch-Supan et al., 2017; Coyle and Cooney, 1993). Oceanic fronts are relatively narrow zones of enhanced horizontal gradients of physical, chemical and biological properties (temperature, salinity, nutrients, plankton communities, etc.) that separate broader areas of different vertical structure (stratification) (Belkin et al., 2009). Upwelling fronts occur in many well studied systems, including the upwelling off southern Senegal, south of Cap-Vert Peninsula known as the "Petite Côte" (14.6°–13.5° North, 16.9°–17.6° West). Senegalese coasts are characterized by a seasonal upwelling (in winter and late spring), mainly driven by wind variability, topography, and density stratification (Estrade et al., 2008). During the upwelling season, northerly trade winds induce a strong upwelling core south of Dakar (Ndoye et al., 2014; Roy, 1998). The upwelling core is located over the shelf, and SST (Sea Surface Temperature) is lowest on the coastal side of the shelf break, increasing in both offshore and coastal directions. Local bottom relief combined with the wind-induced upwelling establish a typical upwelling that appear as a cold-water tongue. This cold-water tongue separates the nutrient-poor warm offshore cell with a cold nutrient-rich coastal cell functioning as a retention zone (Roy, 1998; Tiedemann and Brehmer, 2017). The Petite Côte in the Senegalese coastal shelf is a nursery area for fish and is the main area in which juveniles of numerous species particularly small pelagic species concentrate (Diankha et al., 2018; Thiaw et al., 2017). This area is also known to be rich in zooplankton and micronekton. Many zooplankton groups are encountered over the Senegalese coastal shelf: copepods, amphipods, annelids, appendicularians, chaetognaths, cirrhipeds, cladocerans, decapoda, echinoderms, euphausiids, gasteropods, jellyfish, mysidascea, ostracods, pelagic foraminifera, Protozoa, pteropods, Spumellaria. Copepod is the most dominant group with a total abundance ranging from 50 to 90% (Anonymous, 2013; Ndour et al., 2018; Touré, 1971). Previous study (Ndour et al., 2018; Tiedemann and Brehmer, 2017) on ichthyoplankton showed that Sparidae (~50%) was predominant followed by fewer Engraulidae (~8%) and Soleidae (~7%) while smaller proportions of Clupeidae and Carangidae (~4% each) as well as Myctophidae and Sciaenidae (~2% each) were found. Physical variability in the Senegalese coastal shelf (Capet et al., 2016; Ndoye et al., 2017) can impact marine pelagic organisms at the individual and community level

(Urmy and Horne, 2016). Such impact can be direct via advection or indirect via phytoplankton production fertilized by upwelled nutrients. Indeed, changes in physico-chemical water properties and biological activities induced by upwelling plays a structuring role on the distribution of SSLs. SSLs position is often reported below the thermocline suggesting that temperature controls the SSLs vertical distribution (Aoki and Inagaki, 1992; Baussant et al., 1992; Boersch-Supan et al., 2017; Marchal et al., 1993). Bottom depth has been identified as an additional factor structuring the vertical distribution of SSLs (Gausset and Turrel, 2001). For example, the thickness and depth of an SSL on continental shelves tend to increase with an increase in water depth (Torgersen et al., 1997), similar to patterns observed in the deep sea (Berge et al., 2014; Boersch-Supan et al., 2017). In deep sea areas and over shelves, the maximum density of SSLs are often correlated with maximum chlorophyll-*a* concentrations (Berge et al., 2014; Dekshenieks et al., 2001; Holliday et al., 2010). Dissolved oxygen concentrations (above 1 ml l^{-1} *i.e.* 44.661 mmol m^{-3}) can also predict the lower boundary of SSL density, *e.g.*, in Eastern Boundary Upwelling Systems (EBUS), like the Peruvian coastal upwelling system (Bertrand et al., 2010), and the California coastal upwelling system (Netburn and Koslow, 2015).

In this study, we use acoustic tools (Simmonds and MacLennan, 2005) to examine the fine-scale vertical structure of SSLs (*i.e.*, their depth in the water column, thickness, and density) (Bertrand et al., 2013; Brehmer et al., 2006; Perrot et al., 2018). We use fine spatiotemporal resolution of acoustic data to investigate how the pelagic environment influences SSLs in the EBUS off Senegal during an upwelling event. Our objective was to model variations in SSLs structure relative to physico-chemical characteristics of water masses and their locations on the shelf.

2 Materials and methods

2.1 SSLs acoustics sensing and environmental data

We performed a hydroacoustic survey along the "Petite Côte", south of Cap-Vert Peninsula off Senegal (14.6°–13.5° North, 16.9°–17.6° West). The survey was conducted with the research vessel Antea of the French Institute for sustainable development (IRD-France) during the upwelling season from 6 – 18 March 2013. The Petite Côte is a nursery area for fish and is the main area in which juveniles of numerous species (particularly small pelagic species) concentrate (Diankha et al., 2018; Thiaw et al., 2017). Strong upwelling occurs during spring,

which contributes to high primary productivity, thus providing an ideal nursery area for commercially important fish species (Tiedemann and Brehmer, 2017).

We collected hydroacoustic data along three transects [T1 (North), T2 (intermediary), and T3 (South)] in 18 nautical miles (nmi) perpendicular to the coast (Fig. 1). Hydroacoustic data were continuously recorded (day and night) using a Simrad EK60 echosounder (38, 70, 120 and 200 kHz), set at 20 log R time-varied gain function (R = range in meters) and used a pulse length of 1.0 ms. In this study, we used the acoustic monofrequency approach (using 38 kHz, one of the most current frequencies used in fisheries surveys) to study the spatio-temporal SSLs structure. The 38 kHz frequency offers the advantages of depth-penetration covering the whole vertical range of SSLs. The multifrequency echogram was used to identify the main scatterers of SSLs and to justify the SSLs extraction threshold (see below). Transducers were calibrated following the procedures recommended in Foote et al. (1987). Considering aft draught of the vessel, the acoustic near field and the presence of acoustics parasites (including air bubbles) in the upper part of the water column, we have applied an offset of 10 m (acoustic data above 10m have been deleted). Echoes along the three transects were integrated at a spatial resolution of 0.1 nmi*1m depth. We estimated the SSLs acoustic density by calculating the Nautical Area Scattering Coefficient (NASC or s_A), which represents the relative biomass of acoustic targets. We assumed that the composition of the scattering layers and the resulting scattering properties of organisms in the SSLs are homogeneous within each layer we identified (*sensu* MacLennan et al., 2002). We analyzed integrated echoes using the in-house tool "Matecho" (Perrot et al., 2018). Matecho is an integrative processing software that allows to manually correct echograms (*e.g.*, by correcting bottom depths, removing empty pings, removing echogram interferences, and reducing background noise). For echointegration accuracy, Matecho compute a quality factor (QC) (Fig S1) for each echointegration cell which is the number of integrated samples divided by the total number of sample in one echointegration cell.

After each echogram correction, we extracted the SSLs that were below the mean acoustic volume backscattering strength (S_v in dB) threshold of -75 dB (*i.e.*, values below -75 dB were excluded from the analysis). Cascão et al., (2017) and Saunders et al., (2013) excluded marine pelagic organisms that backscattered at -70 dB, a threshold based on the aggregative behavior of marine pelagic organisms. The SSLs extraction method is based on a threshold of -75 dB and a Matlab algorithm used in Matecho named "contourf.m" (https://ch.mathworks.com/help/matlab/ref/contourf.html), which appear relevant to extract the main SSL at 38 kHz (Fig S2). This process performs a segmentation of the echointegration from the given threshold on echo levels to extract (by calculation of iso-lines according to the

selected S_v threshold) the attached echo groups that formed the SSLs and their associated contours. Based on this contour, a set of descriptors are estimated, e.g., up and down depth of SSL, thickness. In our study, the backscattering was due to zooplankton and micronekton which also include small pelagic fish. The inshore area is known to be rich in copepod and fish larva (Ndour et al., 2018; Tiedemann and Brehmer, 2017) however, low sample number was collected in the coastal inshore water due to safety reason, *i.e.*, research vessel investigate areas of > 20 m bottom depth.

We collected hydrographic data using a calibrated "Seabird SBE19 plus" conductivity, temperature, and depth (CTD) probe. The CTD specifications were: for temperature, $\pm 5.10^{-3}$ °C accuracy and 1.10^{-4} °C precision; for conductivity, $\pm 5.10^{-4}$ S m^{-1} accuracy and 5.10^{-5} S m^{-1} precision; for pressure, ± 0.1% of full-scale range accuracy and 2.10^{-3} % precision of full-scale range precision. The CTD was equipped with sensors for fluorescence ($\pm 2.10^{-3}$ µg l^{-1} accuracy, and $\pm 2.10^{-4}$ µg l^{-1} precision) [a measure of chlorophyll-*a* concentration, a proxy for phytoplankton biomass], and dissolved oxygen (DO, mmol m^{-3}, Seabird SBE43, 2% saturation for accuracy and 0.2% saturation for precision). The CTD have been calibrated before the survey. During the survey data delivered by the SBE43 for DO have been corrected by Winkler titrations. From 6 – 8 March 2013, we conducted CTD casts along three transects at 36 stations. At each station, sensors measured water temperature (°C), depth (m), fluorescence (µg l^{-1}), water density, here sigma-theta (kg m^{-3}), and DO). Global High Resolution Sea Surface Temperature (GHRSST) data were extracted from daily outputs by the Regional Ocean Modeling System group at NASA's Jet Propulsion Laboratory (JPL OurOcean Project, 2010). Daily SST data (GHRSST Level 4 G1SST Global Foundation Sea Surface Temperature Analysis) were averaged for the three days of surveying using SeaDAS software version 7.2 (https://seadas.gsfc.nasa.gov/) and interpolated on maps using R software (R Core Team, 2016). Cubic spline interpolations of gridded data were used within the R package Akima (Akima et al., 2016).

2.2 Data analysis

After extracting SSLs with Matecho, we developed an *ad hoc* Matlab extension of Matecho named "Layer" (Text S1). We obtained SSL thickness, minimum and maximum SSL depths ($D_{min.}$ and $D_{max.}$, respectively) and an echointergrated echogram from Matecho output files to provide it to another Matlab program "ComparEchoProfil" (Text S2). ComparEchoProfil allows to fit in time and depth echointegrated echograms to the associated CTD vertical profiles. We used the equation below to calculate thickness:

198 Thickness = $D_{max.}$ - $D_{min.}$ (1)

199 Mean nautical area backscattering coefficient (s_A, NASC) and mean acoustic volume
200 backscattering strength (S_v , in dB) profiles were based on the average of three ESUs (small-
201 scale elementary sampling unit): the ESU nearest of the CTD position (ESU_{ctd}) as well as
202 previous and following in correspondence with CTD depths (d_n):

203 $$\overline{s_A(d_n)} = \sum_{i=ESU_{ctd}-1}^{i=ESU_{ctd}+1} s_A(i,d_n) \Big/ 3 \quad (2)$$

204 $$\overline{S_v(d_n)} = 10 \times \log_{10}\left(\sum_{i=ESU_{ctd}-1}^{i=ESU_{ctd}+1} 10^{(S_v(i,d_n)/10)} \Big/ 3 \right) \quad (3)$$

205

206 The ComparEchoProfil displayed the profile for S_v in dB over an ESU of 0.1 nmi around
207 each CTD station. The program also allowed us to display acoustic profiles for physico-
208 chemical parameters (temperature, CHL, density, and DO) associated with S_V profiles (Fig. 2).
209 The output included meta information [station ID, station date, station time, latitude and
210 longitude, diel phase (day, night), and bottom depth], all of which we associated with SSLs
211 descriptors [SSL thickness, maximum SSL depth, S_v, and s_A; based on classic fish school
212 descriptors (Brehmer et al., 2007, 2019)] and physico-chemical parameters associated with each
213 SSL.

214 We applied Hierarchical Cluster Analyses (HCA) to discriminate between water masses of
215 inshore and offshore stations over the continental shelf based on CTD data collected at 10 m
216 depth. HCA was based on Euclidean distance and Ward's aggregation method (Ward 1963).
217 We used Principal Component Analysis (PCA) (Chessel et al., 2013) on the same dataset to
218 determine similarities between CTD stations relative to environmental parameters. Physico-
219 chemical parameters were standardized *a-priori* because they were measured with different
220 metrics.

221 Inshore - offshore variability of morphometric (thickness, depth) and acoustic characteristics
222 (s_A) of the SSLs are investigated in the discriminated groups considering bottom depth and diel
223 period. Diel transition periods are removed from analyses to avoid SSL density changes bias
224 due to diel vertical migrations. Transition periods are defined using sun altitude, *i.e.*, around
225 sunset and sunrise corresponding to a sun altitude between ±18° (Lehodey et al., 2015).
226 Morphometric and acoustic characteristics of the SSLs are also compared between the inshore

area *versus* offshore area, and between day and night using student's t-test whose application conditions density have been verified (normal distribution and variance equality).

Echogram *vs*. profile coupling figures (Fig. 2) resulting from the "ComparEchoProfil" were analyzed to determine the relation between environmental parameters and SSLs. ANCOVA tests (analysis of covariance) (Wilcox, 2017) were implemented for SSLs characteristics (thickness, depth, and density) in each discriminated area (inshore and offshore). These models were set to predict each descriptors, *i.e.*, thickness, depth, and s_A as function of temperature, density, DO, CHL, local depth and diel period. The ANCOVA models were developed on averaged data over station. The selection of the best models was performed using stepwise procedures. Stepwise selection was based on minimizing the Akaike Information Criteria (AIC) (Akaike, 1974). The relative importance of each variable in total deviance explained was determined from the "relaimpo" R package (Tonidandel and LeBreton, 2011). Validity assumptions of the models was then assessed by checking for normality of distributed errors and homogeneity of residuals (Fig S3 to Fig S5). For the ANCOVA, SSL density ($s_{A)}$ was $\log_{10}$ transformed for normality assumption. For all statistical tests, the significance threshold used was 0.05.

We used R software (R Core Team, 2016) for statistical analyses and to map data. We used the R package 'Cluster' (Maechler et al., 2014) for HCA of CTD data, the R package 'maps' (Brownrigg, 2016) to map stations, the package 'ade4' (Chessel et al., 2013) to run a PCA, and the package 'oce' (Kelley, 2015) to display vertical section plots of physico-chemical parameters.

3 Results

3.1 Characterization of two water masses over the shelf

The HCA differentiated two groups of stations (Fig. 3a): Group 1 (G1) stations (n = 18) comprised four stations along transect T1, six stations along transect T2, and eight stations along transect T3. The stations of G1 were located closest to the coast (inshore area, from 13 to 61 m bottom depth, which encompassed the core of the upwelling (based on data for sea surface temperature) (Fig. 1). Group 2 (G2) stations (n = 18) comprised seven stations along transect R1, six stations along transect R2, and five stations along transect R3. These stations were located furthest from shore (offshore area), from 41 to 205 m bottom depth, which corresponds to the outer border of the upwelling zone. Considering the bathymetry, we note an overlay of the two areas discriminated between 41 to 61 m.

PCA identified the same two distinct water masses that were clustered in HCA (Fig. 3). Axis 1 of the PCA eigenvalues explained 72.8 % of the inertia, whereas axis 2 explained 26.8 %. On axis 1 of the PCA plot, temperature was highly correlated with density. On axis 2, temperature, and DO were opposed to CHL. The distribution of these variables is related to the station groupings: G1 (inshore area) was characterized by a dense and CHL-rich water mass, whereas G2 (offshore area) was characterized by a warm and slightly oxygenated surface water mass.

Satellite measurements of SST distributions of the study area indicated the same split of stations into two groups (Fig S6). The inshore area was characterized by low SST values (18 – 19 °C), indicating a recently upwelled water mass, whereas an older water mass with higher SST values (20 – 21 °C) prevailed offshore.

At transect T1, a marked frontal zone appeared isolating two water masses between the 20 – 40 m isobaths (Fig. 4a1) which separated warm surface waters from deep cold upwelled water masses. At transects T2 and T3, the upwelling appeared as a cold-water tongue isolating a warm water band at the coast (Fig. 4a2, a3). At T3, this cold-water tongue was expanding toward the inshore area as well as to the offshore area (Fig. 4a3). Surface water masses of the inshore area were slightly denser than water masses in offshore area with approximately 26 kg m^{-3} and 25 kg m^{-3}, respectively. For CHL, elevated concentrations were exclusively observed in the inshore area at transects T1 and T2. CHL was significantly higher in the inshore area than the offshore area with concentrations of 3.0 – 5.0 mg m^{-3} in the inshore area to 0.3 – 2.0 mg m^{-3} in the offshore area (Fig. 4c). At T3, the elevated CHL concentrations were observed in both inshore and offshore area close to the upwelling front. CHL was higher in the upper part of the water column (0 – 20 m) decreasing with depth in both areas. Higher DO concentrations were observed towards both sides of the upwelling core. At T1, the upwelling front was at the most coastal part separating the inshore area from the less oxygenated offshore area with DO concentrations of 223 – 312 mmol $m^{-3}$and 178 – 223 mmol m^{-3}, respectively. At T2 and T3, the core moved towards the offshore, separating the inshore area (DO concentrations of 178 – 223 mmol m^{-3}) slightly more oxygenated than the offshore area (DO concentrations of 89 – 178 mmol m^{-3}). DO concentration decreased from the surface to bottom in both areas.

3.2 Variability in vertical structure of SSLs

3.2.1 Spatial variability according to water mass characteristics

Thickness and depth of the SSLs varied according to bottom depth in the inshore area and the offshore area. In the inshore area, on the northern transect T1, no SSLs were observed at coastal stations shallower than 29 m bottom depth (stations 1 and 2) (Fig. 5a). In offshore

stations, starting at 41 m bottom depth, the SSLs were observed in all stations and transects (Fig. 5b), and their thickness and depth increased with bottom depth. SSL thickness and SSL depth differed significantly between the inshore area and the offshore area: the SSLs were thicker and deeper in the offshore area than in the inshore area (Fig. 6) (p-value = 0.001 for both thickness and depth). An increase of SSL was observed with increasing bottom depths in the inshore area and the offshore area. The s_A comparison between the inshore area and the offshore area (Fig. 6) was not significantly different (p-value = 0.833).

3.2.2 Diel migration

The diel period had a significant effect on SSL thickness (p-value < 0.001), and SSL depth (p-value < 0.001) which were found both higher during the night in the inshore area and the offshore area (Fig. 6). In the inshore area, during daytime, the mean depth and thickness of SSL were 19 and 11 m respectively, while during night, the mean depth and thickness were 46 and 35 m respectively. In the offshore area, SSLs were found at a mean depth and thickness of 49 and 38 m, respectively during daytime, while during night-time SSLs, depth and thickness were 86 and 75 m, respectively. Mean s_A (Fig. 6) of SSLs varied also between day and night but were not significantly different (p-value = 0.890). In the inshore area, the mean s_A was 24 m^2 nmi^{-2} during the day and 44 m^2 nmi^{-2} during the night. In the offshore area, the mean s_A was 46 m^2 nmi^{-2} during daytime, and 25 m^2 nmi^{-2} during night-time. Mean S_v distribution of SSLs (Fig S7) showed also a diel variation with mean Sv higher at night than during the day.

3.2.3 Vertical dimension of SSLs related to physico-chemical profile

In both areas, SSLs were partially or completely located in areas of strong vertical gradients of temperature (thermocline), density (pycnocline), and DO (oxycline) (Fig. 2). When a strong temperature gradient, usually also associated to the vertical position of the oxycline and a pycnocline, a peak of CHL was often observed and matched with the volume backscattering strength (S_v) peak (Fig. 2a). This observation is well illustrated in CTD stations 12, 13, 16, and 25 (Fig S8). In the inshore area, the peak of CHL concentration was always located above the SSLs (Fig. 2a), whereas in the offshore area, the peak of CHL concentration was either above the SSLs or in the middle of the SSLs (Fig. 2b). The thickest SSLs were observed in the offshore area where temperature, density, and oxygen gradient were strong.

3.2.4 Behavior of the SSLs relative to pelagic habitat characteristics

3.2.4.1 In the inshore area (G1)

In the inshore area (G1), the ANCOVA model indicated a strong effect of bottom depth and diel period on both SSLs thickness and depth. For SSL thickness, the model (Table 1) explained 87 % of the variance (R^2 = 0.869, *p*-value = 0.001). Bottom depth explained 56 % of SSL thickness while the diel period effect accounted for 31 %. The model of SSL depth (Table 2) was like those of SSL thickness, *i.e.*, the model included bottom depth and diel period explaining 80 % of the variance (R^2 = 0.805, *p*-value = 0.001). Bottom depth showed the largest effect on SSLs explaining 51 % of SSL depth while the diel period effect was estimated at 30 %. For SSL acoustic density, *i.e.*, log (s_A) (Table 3), the model explained 40 % of the variance (R^2 = 0.398, *p*-value=0.022) indicating a single effect of bottom depth on log (s_A) (*p*-value = 0.020). The bottom depth was the only variable significant in the model and explained 33 % of SSL acoustic density. Temperature was insignificant in the model.

The ANCOVA models to predict SSL thickness and SSL depth can be expressed as:

$$SSL_{thickness} = -11.865 + (0.916 * B_d) + (11.492 * D_p)$$

$$SSL_{depth} = -4.223 + (0.954 * B_d) + (12.864 * D_p)$$

With B_d= Bottom depth in m; D_p = Diel period in night;

3.2.4.2 In the offshore area (G2)

For offshore stations, the model showed a significant effect of diel period, temperature, water density and DO on both thickness and depth of SSLs with similar results. Both models, SSL thickness (Table 1) and SSL depth (Table 2) included bottom depth, diel period, temperature, density, and DO explaining 85 % of variance (R^2 = 0.855, *p*-value = 0.001). Bottom depth and diel period accounted for 28 % and 28 %, respectively. Other significant variables were water temperature, density, and DO, which support 11 %, 10 %, and 7 %, respectively. For SSL density or log(s_A) (Table 3), none of the predictor variable had a significant effect.

The ANCOVA models to predict SSL thickness and SSL depth can be expressed as:

$$SSL_{thickness} = 56030 + (0.21 * B_d) + (27.35 * D_p) + (-383.80 * T) - (1898 * D) - (1.76 * O_2)$$

$$SSL_{depth} = 56040 + (0.21 * B_d) + (27.35 * D_p) + (-383.80 * T) - (1898 * D) - (1.76 * O_2)$$

With B_d= Bottom depth in m; D_p = Diel period in night; T = Water Temperature in °C;

D = Water Density in kg m^{-3}; O_2= oxygen in mmol m^{-3}.

4 Discussion

4.1 Characterization of water masses along the Petite Côte

Upwelling is a key process in the functioning of the coastal ecosystem of Senegal and Mauritania (Capet et al., 2016; Estrade et al., 2008; Rebert, 1983). By characterizing the physico-chemical parameters of the Petite Côte, we were able to discriminate two water masses, an inshore area and the offshore area, both of which could also be distinguished with SST satellite data.

Analyzing the spatial structure of SST helped to understand the upwelling dynamics along the Petite Côte. The SST pattern, measured at the time of our survey, were in line with prior studies. During the upwelling season (in winter and late spring), a tongue of cold water over the shelf isolates a coastal band of warm water from the offshore area, and there is a surface separation associated with the upwelling source over the shelf and convergence nearshore. The spatial difference of CHL concentration between the inshore area and the offshore area is the result of upwelled water carrying nutrients to the coast, which is separated by water mass fronts. Nutrient-rich water, supplied to the sunlit surface layer by wind-driven upwelling stimulates the growth of phytoplankton that ultimately fuel diverse and productive marine ecosystems (Jacox et al., 2018). There is a link between the accumulation of biological material and the location of the coastal band of warm water. This coastal band between coast and the upwelling core has been regarded to function as retention area in which nutrient particles are trapped (Demarcq and Faure, 2000; Roy, 1998). The nutrient utilization is optimized by retentive physical mechanisms in the coastal area, which enhances microbial remineralization of particulate organic matter and zooplankton excretion, and then regenerates production through ammonium consumption (Auger et al., 2016). This causes an increase in primary production and results in a surplus of phytoplankton biomass in inshore areas. Low DO concentrations observed in the upwelling core separating more oxygenated water masses have been reported in previous studies (Capet et al., 2016; Teisson, 1983) over the Petite Côte. Once a water mass becomes isolated from the atmosphere, its oxygen content starts to decrease due to biological remineralisation of dissolved organic matter (Emerson et al., 2008; Machu et al., 2019). These low-oxygen bottom waters are transported to the inner shelf during upwelling favourable wind events. Moreover, temporal stability of the upwelling core is also noticeable over periods of several days to weeks; and export from the shelf to the open ocean is retarded (Capet et al., 2016). Thus, in such favorable condition of continuous food supply, photosynthesis may foster

an enrichment of DO in the inshore. This is in line with high CHL levels observed towards both side of upwelling core, particularly in the inshore area.

4.2 Spatial variation of the SSLs off the Petite Côte of Senegal

We measured a longitudinal gradient in the thickness of the SSLs over the continental shelf. The SSLs were concentrated in a narrow band in the inshore area, whereas the SSLs were wider in the offshore zone. The absence or weakness of SSLs in the inshore area (in contrast to the more stratified water column in the offshore area) may have been due to turbulence in the water column (Sengupta et al., 2017), coupled with well-mixed surface layer. In the inshore area, it is likely that turbulence and the probable low residence time of marine pelagic organisms advected from outside this area, both inhibited SSLs formation. Indeed, in such upwelling systems, in addition to the retention mechanism that has been recognized by several authors (Arístegui et al., 2009; Capet et al., 2016; Mbaye et al., 2015; Roy, 1998), there is also an offshore Ekman transport mechanism (Arístegui et al., 2009; Estrade et al., 2008) that contribute to cross-shore exchanges. Otherwise, different animals can respond very differently to different physical forcing. Many authors have stressed that SSLs need stable hydrological conditions to form (Aoki and Inagaki, 1992; Baussant et al., 1992; Marchal et al., 1993). As example, in Monterey Bay (California), Urmy and Horne (2016) observed a decline in acoustic backscatter intensity in the upper part of the water column immediately following an upwelling event. In a more recent study, Benoit-Bird et al (2019) found that when upwelling was strong, both krill and anchovies were found in small, discrete aggregations, while during upwelling relaxation and reversals, forage biomass was more diffusely distributed. Therefore, we assume that the increase of SSL thickness with depth from inshore to offshore off Senegal is caused by upwelled waters that disrupt the vertical stability of the water column. Therefore, although the SSLs are first constrained by the bottom depth (*i.e.*, room available), we assume that the increase of SSL thickness with depth from inshore to offshore off Senegal is caused by upwelled waters that disrupt the vertical stability of the water column.

4.3 Diel temporal variation of SSLs

In our study area, the diel period consistently exhibited pronounced effects on SSLs thickness and depth. Deeper night SSLs have a greater thickness than daytime SSLs. The diel difference of thickness and depth is due to the well-known DVM patterns performed by many marine species. DVM is a behavioural mechanism usually characterized by an ascent during night-time for feeding and a descent to avoid predation by visual predators during daytime

known as type I (Bianchi et al., 2013; Haney, 1988; Lehodey et al., 2015). Some plankton and micronekton organisms have been reported to exhibit reverse DVM (type II), *i.e.*, ascending in the morning and descending in the evening or early night, which is the opposite pattern generally observed with vertically migrating animals (Cushing, 1951; Ohman et al., 1983). The main SSL scatters much more strongly at 38 kHz than at 70 or 120 kHz (Fig. 2) the backscattering response is probably dominated by swimbladdered animals such as fish larvae and small fish (Simmonds and MacLennan, 2005). Indeed, the Petite Côte is a nursery area for fish and is the main area in which juveniles of numerous species concentrate (Diankha et al., 2018; Thiaw et al., 2017). Moreover Tiedemann and Brehmer (2017) have reported fish larvae (*Sardinella aurita, Engraulis encrasicolus, Trachurus trachurus, Trachurus trecae, Microchirus ocellatus* and *Hygophum macrochi*) all along our study area. Previous studies reported that DVM of plankton may increase coastal retention in the inshore area (Brochier et al., 2018; Mbaye et al., 2015; Rojas and Landaeta, 2014a). Diel variation was also observed for SSL acoustic density, which showed opposite patterns in the two areas, *i.e.*, higher up in the water column during night than day in the inshore area and higher up during days than at night in the offshore area. Tiedemann and Brehmer (2017) observed that all fish larvae in the offshore area, except *Trachurus trachurus*, exhibited a DVM type II, and their observations are in accordance with the DVM pattern of SSL acoustic density reported in our study. Another possible explanation of this observed diel variation is the horizontal migration. DHM are known as nocturnal horizontal migration of both plankton and consumers into shallow and inshore waters (Benoit-Bird et al., 2001; Benoit-Bird and Au, 2006). DHM have been observed in marine copepods (Suh and Yu, 1996) which represent the main zooplankton group in the study area (Ndour et al., 2018; Rodrigues et al., 2017). It is hypothesized that these inshore–offshore migrations are a strategy for avoiding visual predators (White, 1998), and result in increased access to food resources relative to simple vertical migration (Benoit-Bird et al., 2008). Otherwise, DVM of marine pelagic organisms may not be the only factors causing diel backscatter variations. (i) The acoustic target strength can be strongly dependent on the aspect at which a target is insonified. Target strengths of zooplankton and micronekton can vary by several orders of magnitude between extreme tilt angles, *i.e.*, horizontal *vs*. head up or head down (Benoit-Bird and Au, 2004; Yasuma et al., 2003). Target strength is not independent of depth, as migrations through the hydrostatic depth gradient can alter, *e.g.*, swim bladder volume (Fässler et al., 2009). This can bias target strengths, in particular near the resonance frequency, leading to artificial increases of backscatter at a particular depth (Davison et al., 2015; Godø et al., 2009; Kloser et al., 2002). (ii) in the inshore area the CTD sampling was mainly achieved

during the daytime, which may have biased the observed DVM type I. (iii) Otherwise, plankton such as fish larvae are able to perform a DVM type II by ascending in the upper 10 m of the water column at night, *i.e*., in the echosounder offset.

4.4 Effect of environmental parameters on SSLs

4.4.1 SSLs related to physico-chemical parameters in the vertical dimension

Previous studies have shown that hydrographic structures of the water column influence SSLs vertical structure (Balino and Aksnes, 1993; Berge et al., 2014; Gausset and Turrel, 2001). In our case study the results show that vertical distribution of SSLs was linked to strong vertical gradients of temperature, DO, and water density (Fig. 2). The peak of S_v were sometimes very close to the strong gradient of water temperature, density, CHL and DO (Fig S8). The depth of SSLs has been reported to be related to thermocline (Marchal et al., 1993; Yoon et al., 2007). In more stratified areas, SSLs vertical distribution was limited by a strong thermocline and when thermocline was not well marked (low gradient), SSLs occupied the entire water column (Lee et al., 2013). Olla and Davis (1990) and Rojas and Landaeta (2014b) suggeted that thermocline is a physical barrier that acts above or below in the vertical distribution of some fish larvae while other studies (Gray and Kingsford, 2003; Tiedemann and Brehmer, 2017) showed no effect of a thermocline on vertical larval fishes distribution. In this study, the SSL was correlated to temperature in the offshore stratified area, but didn't act as a physical barrier limiting vertical distribution. Previous studies (Bertrand et al., 2010; Bianchi et al., 2013; Netburn and Koslow, 2015) have suggested that vertical distributions of SSLs organisms are limited by mid-water DO concentrations which constraint SSLs depth. These authors found a relationship between SSLs depths and hypoxia. However, in our study, we found correlation between SSLs (depth, thickness) and DO as expected, but vertical distribution of SSLs was not constrained by DO. SSLs was also observed in some hypoxic stations (DO <1.42 ml l^{-1} i.e. 63.42 mmol m^{-3}), consequently, DO was not a limiting factor for SSLs organisms. Fish larvae respond to oxygen gradients by moving upwards or laterally (Breitburg, 2002; 1994). Vertical movement of fish larvae may be also related to the avoidance of predators, which are limited to well oxygenated layers. The high phytoplankton concentration found in this study, particularly in the inshore area may be interpreted as a potential food source for fish larvae, which are able to perform DVM towards the surface. The vertical position of SSLs compared to the CHL concentration peak can be explained by trophic relationships between phytoplankton, zooplankton, and micronekton. It is understood that zooplanktivorous micronekton migrates upward in the water column to forage on mesozooplankton while the mesozooplankton at the

same time is migrating toward the surface to graze upon the phytoplankton. This trophic relationship may explain the link in vertical position of the SSLs with the phytoplankton peak reported in this study.

4.4.2 Behavior of SSLs relative to pelagic habitat characteristics

In the inshore area, where SSLs were sparsely present (or sometimes non-existent) bottom depth and diel period were the main environmental parameters influencing the vertical distribution (thickness and depth) of the SSLs. Bottom depth has been shown to regulate the vertical distribution of SSLs in the water column (Donaldson, 1967; Gausset and Turrel, 2001; Torgersen et al., 1997). In our study, all stations indicated a single SSL, while in deep water more thick and deep SSLs are often partitioned into multiple layers (Ariza et al., 2016; Balino and Aksnes, 1993; Cascão et al., 2017; Gausset and Turrel, 2001). Diel period is the second most important parameter acting on SSL thickness and depth through the DVM phenomenon. In well mixed water masses, temperature, density, and oxygen had no effect on the SSLs. The insignificant effect of temperature, oxygen, and water density on the SSLs in the inshore area is explained by the presence of less marked and superficial clines because of the newly upwelled water. As stated above, SSLs need probably stable condition to occur.

In the offshore area, where vertical gradients were marked, the main parameters structuring SSL thickness and depth were bottom depth and diel period, but also water temperature, density and DO. DVM behaviors are influenced by environmental cues (*e.g.*, light, nutrients, and temperature) and predator-prey interactions (Clark and Levy, 1988; Lampert, 1989). Relative changes in light intensity are identified as the most important proximate stimuli driving DVM, including the amplitude of the migration as well the timing of the up and downward movement (Meester, 2009). SSLs vertical distribution is known also to be a function of temperature (Bertrand et al., 2010; Hazen and Johnston, 2010; Netburn and Koslow, 2015). Overnight, depth of SSLs is strongly correlated to the depth of thermal and density gradients (Boersch-Supan et al., 2017; Cascão et al., 2017; Marchal et al., 1993). In the offshore area, the results suggest that DO also influence SSL depth and SSL thickness. In well oxygenated continental shelf waters, DO influences SSLs but do not limit their vertical distribution. Some previous work in French Polynesia (Bertrand et al., 2000), and in the southern California current ecosystem (Netburn and Koslow, 2015) showed that the oxygen minimum zone (OMZ) act like a barrier of SSLs in their vertical distribution. Bianchi et al., (2013) suggest that distribution of open-ocean OMZ may modulate the depth of migration at the large scale, so that organisms within SSLs migrate to shallower waters in low-oxygen regions, and to deeper waters in well-oxygenated waters.

For both areas, CHL concentration was the only predictor that was not included in any of the final models. However, coupling echogram *vs*. profile (Fig. 2), we can argue that a relation between CHL and SSLs exists even if it was not significant in the models, because CHL and SSL biomass peaks matched, *i.e*., always located above or in the middle of the SSLs. Moreover, simple linear model between CHL and SSLs structure (depth and thickness) was significant in the inshore area, suggesting that CHL effect on full models was masked by autocorrelation between predictive variables.

Fish larvae vertical distribution have been related to the distribution of their prey and predator, and it has been argued that the presence and position of the thermocline is an important feature in their vertical distribution (Haney, 1988; Röpke, 1993). Other studies have shown that thermocline has only a limited role in the vertical distribution patterns of fish larvae (Gray, 1996; Gray and Kingsford, 2003). Indeed, in coastal areas, where the structure of the water column is less regular than in the open sea, vertical distribution of fish larvae depends on the physics of the water column (Sánchez-Velasco et al., 2007) but also on the behavior of each species (Fortier and Harris, 1989). According to Sánchez-Velasco et al. (2007), vertical distribution of fish larvae is closely related to the changes of the water column structure, with most fish larvae concentrated in the stratum of maximum stability. Therefore, the vertical stratification level in water column is strongly related to vertical distribution of these organisms.

Furthermore, the vertical distribution of SSLs can be influenced by mixed layer depth (MLD). The MLD is one of the primary factors affecting the vertical distribution of zooplankton. Lee et al. (2018) have shown that the weighted mean depths of SSLs exhibit a strong linear relationship with the MLD, meaning that the MLD could be a significant environmental factor controlling the habitat depth of marine pelagic organisms. A recent study (Stranne et al., 2018) has shown that the MLD can be tracked acoustically at high horizontal and vertical resolutions. The method was shown to be highly accurate when the MLD is well defined and biological scattering does not dominate the acoustic returns. However, in our study area, biological scattering dominated the acoustic records and due to the upwelling acoustic methods were not appropriate to determine MLD.

5 Conclusion

Using our echogram *vs.* profile coupling approach, we were able to examine fine-scale processes affecting SSLs distribution. SSLs were influenced by turbulence level in the upwelling, which lead to an offshore advection of SSLs organisms. SSLs distribution were mainly structured by bottom depth, diel period, and the level of vertical stratification in water

column. SSL acoustic density variation suggested different diel migrations: a normal and reverse DVM, and/or a DHM. Such observation should be considered in modelling exercise to better understand DVM implication in ecosystem functioning. Further investigations should integrate small-scale turbulence measurements to better describe the fine scale spatiotemporal variability of SSLs and their relationship to the pelagic environment. Information on SSL species composition and morphological characteristics will provide accurate description of their fine scale relationship to pelagic habitat.

6 Software and Code availability

"Matecho" is an Open-Source Tool available at: https://svn.mpl.ird.fr/echopen/MATECHO/ (login: userecho, password: echopen). Other Matlab codes used in this work: "Layer" and "ComparEchoProfil" are shared in the Supplement material B and C of this paper.

7 Sample availability

The public cannot access our data because they belong to the partners who funded the oceanographic cruise.

8 Author contribution

Ms. Ndague DIOGOUL set the methodology, analysed data and redacted the paper and the review. Patrice BREHMER was cruise leader on the ECOAO sea survey, defined the sampling design, collected the data, defined the methodology, supervised the work and the review and took charge of the acquisition of the financial support for the project leading to this publication. Maik TIEDEMANN helped on data processing and analyses, paper redaction and the review. Yannick PERROT developed the "Matecho" software tool and Matlab code, contributed to the redaction and data collection as Abdoulaye SARRÉ. Abou THIAM, and Salaheddine EL AYOUBI contributed to the Ndague DIOGOUL PhD supervision. Anne MOUGET and Chloé MIGAYROU helped on statistical analyses and Oumar SADIO performed the early PCA on CTD data.

9 Acknowledgments

Results of this paper were discussed during international conferences (ICAWA) in Dakar (2016) and in Mindelo (2017). We thank the participants for helpful comments made during these conferences. We are thankful to the AWA project (Ecosystem Approach to Management of Fisheries and Marine Environment in West African Waters) funded by IRD and the BMBF (grant 01DG12073E), and the PREFACE project (Enhancing Prediction of Tropical Atlantic Climate and its Impacts) funded by the European Commission's Seventh Framework Programme under Grant Agreement number 603521 and then the TriAtlas project (GA n. 817578; EU H2020 R&I programme), and all IRD - ISRA/CRODT - Genavir staff helping us at sea during the survey (doi: 10.17600/13110030). We thank Gildas Roudaut, Fabrice Roubaud, François Baurand and the US Imago (IRD) for data collection on-board FRV Antea (IRD), the Gnavir crew of Antea, Dominique Dagorne (IRD) curating satellite products, as well as the personal of ISRA/CRODT (Senegal), IRD DR-Ouest (France) and INRH (Morocco) for their administrative help during Ms. Ndague Diogoul PhD stays in Morocco financed by OWSD (Organization for Women in Sciences for the Developing World). We thank Dr Heino Fock (TI, Germany) for his helpful comments on this works paper which significantly improve the paper quality, as well as anonymous referee.

10 References

Akaike, H.: A new look at the statistical model identification, IEEE Trans. Autom. Control, 19(6), 716–723, doi:10.1109/TAC.1974.1100705, 1974.

Akima, H., Gebhardt, A., Petzold, T. and Maechler, M.: akima: Interpolation of Irregularly and Regularly Spaced Data. [online] Available from: https://CRAN.R-project.org/package=akima (Accessed 8 July 2018), 2016.

Anonymous: Rapport des travaux de recherches scientifiques à bord du navire « ATLANTIDA » réalisés dans la Zone Economique Exclusive (ZEE) du Sénégal (Décembre 2012)., Rap. Scient., AtlantNiro, Russie., 2013.

606 Aoki, I. and Inagaki, T.: Acoustic observations of fish schools and scattering layers in a
607 Kuroshio warm-core ring and its environs, Fish. Oceanogr., 1(2), 137–142, 1992.

608 Arístegui, J., Barton, E. D., Álvarez-Salgado, X. A., Santos, A. M. P., Figueiras, F. G., Kifani,
609 S., Hernández-León, S., Mason, E., Machú, E. and Demarcq, H.: Sub-regional ecosystem
610 variability in the Canary Current upwelling, Prog. Oceanogr., 83(1), 33–48,
611 doi:10.1016/j.pocean.2009.07.031, 2009.

612 Ariza, A., Landeira, J. M., Escánez, A., Wienerroither, R., Aguilar de Soto, N., Røstad, A.,
613 Kaartvedt, S. and Hernández-León, S.: Vertical distribution, composition and migratory
614 patterns of acoustic scattering layers in the Canary Islands, J. Mar. Syst., 157, 82–91,
615 doi:10.1016/j.jmarsys.2016.01.004, 2016.

616 Auger, P.-A., Gorgues, T., Machu, E., Aumont, O. and Brehmer, P.: What drives the spatial
617 variability of primary productivity and matter fluxes in the north-west African upwelling
618 system? A modelling approach, Biogeosciences, 13(23), 6419–6440, doi:10.5194/bg-13-6419-
619 2016, 2016.

620 Balino, B. and Aksnes, D.: Winter distribution and migration of the sound scattering layers,
621 zooplankton and micronekton in Masfjorden, western Norway, Mar. Ecol.-Prog. Ser., 102, 35–
622 50, doi:10.3354/meps102035, 1993.

623 Baussant, T., Ibanez, F., Dallot, S. and Etienne, M.: Diurnal mesoscale patterns of 50-khz
624 scattering layers across the ligurian sea front (NW mediterranean-sea), Oceanol. Acta, 15(1),
625 3–12, 1992.

626 Belkin, I. M., Cornillon, P. C. and Sherman, K.: Fronts in Large Marine Ecosystems, Prog.
627 Oceanogr., 81(1), 223–236, doi:10.1016/j.pocean.2009.04.015, 2009.

628 Benoit-Bird, K., Au, W., E. Brainard, R. and Lammers, M.: Diel horizontal migration of the
629 Hawaiian mesopelagic boundary community observed acoustically, Mar. Ecol. Prog. Ser., 217,
630 1–14, doi:10.3354/meps217001, 2001.

631 Benoit-Bird, K. J. and Au, W. W. L.: Diel migration dynamics of an island-associated sound-
632 scattering layer, Deep Sea Res. Part I: Oceanogr. Res. Pap., 51(5), 707–
633 719,doi:10.1016/j.dsr.2004.01.004, 2004.

634 Benoit-Bird, K. J. and Au, W. W. L.: Extreme diel horizontal migrations by a tropical nearshore
635 resident micronekton community, Mar. Ecol. Prog. Ser., 319, 1–14, doi:10.3354/meps319001,
636 2006.

637 Benoit-Bird, K. J., Zirbel, M. J. and McManus, M. A.: Diel variation of zooplankton
638 distributions in Hawaiian waters favors horizontal diel migration by midwater micronekton,
639 Mar. Ecol. Prog. Ser., 367, 109–123, doi:10.3354/meps07571, 2008.

640 Benoit-Bird, K. J., Waluk, C. M. and Ryan, J. P.: Forage Species Swarm in Response to Coastal
641 Upwelling, Geophys. Res. Lett., 46(3), 1537–1546, doi:10.1029/2018GL081603, 2019.

642 Berge, J., Cottier, F., Varpe, O., Renaud, P. E., Falk-Petersen, S., Kwasniewski, S., Griffiths,
643 C., Soreide, J. E., Johnsen, G., Aubert, A., Bjaerke, O., Hovinen, J., Jung-Madsen, S., Tveit, M.
644 and Majaneva, S.: Arctic complexity: a case study on diel vertical migration of zooplankton, J.
645 Plankton Res., 36(5), 1279–1297, doi:10.1093/plankt/fbu059, 2014.

Bertrand, A., Misselis, C., Josse, E. and Bach, P.: Caractérisation hydrologique et acoustique de l'habitat pélagique en Polynésie française : conséquences sur les distributions horizontale et verticale des thonidés, in Les espaces de l'Halieutique, Actes du quatrième Forum Halieumétrique, pp. 55–74, Gascuel, D., Biseau, A., Bez, N. and Chavance, P., Paris. [online] Available from: http://horizon.documentation.ird.fr/exl-doc/pleins_textes/divers09-03/010024490.pdf, 2000.

Bertrand, A., Ballón, M. and Chaigneau, A.: Acoustic Observation of Living Organisms Reveals the Upper Limit of the Oxygen Minimum Zone, PLOS ONE, 5(4), e10330, doi:10.1371/journal.pone.0010330, 2010.

Bertrand, A., Grados, D., Habasque, J., Fablet, R., Ballon, M., Castillo, R., Gutierrez, M., Chaigneau, A., Josse, E., Roudaut, G., Lebourges-Dhaussy, A. and Brehmer, P.: Routine acoustic data as new tools for a 3D vision of the abiotic and biotic components of marine ecosystem and their interactions, in 2013 IEEE/OES Acoustics in Underwater Geosciences Symposium, RIO Acoustics, doi: 10.1109/RIOAcoustics.2013.6683995, 2013.

Bianchi, D., Stock, C., Galbraith, E. D. and Sarmiento, J. L.: Diel vertical migration: Ecological controls and impacts on the biological pump in a one-dimensional ocean model, Glob. Biogeochem. Cycles, 27(2), 478–491, doi:10.1002/gbc.20031, 2013.

Boersch-Supan, P. H., Rogers, A. D. and Brierley, A. S.: The distribution of pelagic sound scattering layers across the southwest Indian Ocean, Deep Sea Res. Part II Top. Stud. Oceanogr., 136, 108–121, doi:10.1016/j.dsr2.2015.06.023, 2017.

Brehmer, P., Lafont, T., Georgakarakos, S., Josse, E., Gerlotto, F. and Collet, C.: Omnidirectional multibeam sonar monitoring: Applications in fisheries science, Fish and Fisheries, 7, 165–179, doi:10.1111/j.1467-2979.2006.00218.x, 2006.

Brehmer, P., Georgakarakos, S., Josse, E., Trygonis, V. and Dalen, J.: Adaptation of fisheries sonar for monitoring schools of large pelagic fish: dependence of schooling behaviour on fish finding efficiency, Aquat. Living Resour., 20(4), 377–384, doi:10.1051/alr:2008016, 2007.

Brehmer, P., Sarré, A., Guennégan, Y. and Guillard, J.: Vessel Avoidance Response: A Complex Tradeoff Between Fish Multisensory Integration and Environmental Variables, Rev. Fish. Sci. Aquac., 27(3), 380–391, doi:10.1080/23308249.2019.1601157, 2019.

Brehmer, P. A. J.-P.: Fisheries Acoustics: Theory and Practice, 2nd edn, Fish and Fisheries, 7(3), 227–228, doi:10.1111/j.1467-2979.2006.00220.x, 2006.

Breitburg, D.: Effects of hypoxia, and the balance between hypoxia and enrichment, on coastal fishes and fisheries, Estuaries, 25(4), 767–781, doi:10.1007/BF02804904, 2002.

Breitburg, D. L.: Behavioral response of fish larvae to low dissolved oxygen concentrations in a stratified water column, Mar. Biol., 120(4), 615–625, doi:10.1007/BF00350083, 1994.

Brochier, T., Auger, P.-A., Pecquerie, L., Machu, E., Capet, X., Thiaw, M., Mbaye, B. C., Braham, C.-B., Ettahiri, O., Charouki, N., Sène, O. N., Werner, F. and Brehmer, P.: Complex small pelagic fish population patterns arising from individual behavioral responses to their environment, Prog. Oceanogr., 164, 12–27, doi:10.1016/j.pocean.2018.03.011, 2018.

687 Brownrigg, R.: Package ‘maps’. Available: http://cran.r-project.org/web/packages/maps/
688 [2016-04-01], 2016.

689 Capet, X., Estrade, P., Machu, E., Ndoye, S., Grelet, J., Lazar, A., Marié, L., Dausse, D. and
690 Brehmer, P.: On the Dynamics of the Southern Senegal Upwelling Center: Observed Variability
691 from Synoptic to Superinertial Scales, J. Phys. Oceanogr., 47(1), 155–180, doi:10.1175/JPO-
692 D-15-0247.1, 2016.

693 Cascão, I., Domokos, R., Lammers, M. O., Marques, V., Domínguez, R., Santos, R. S. and
694 Silva, M. A.: Persistent Enhancement of Micronekton Backscatter at the Summits of Seamounts
695 in the Azores, Front. Mar. Sci., 4:25, doi:10.3389/fmars.2017.00025, 2017.

696 Chessel, D., Dufour, A.-B., Dray, S., Jombart, T., Lobry, J. R., Ollier, S. and Thioulouse, J.:
697 ade4: Analysis of Ecological Data: Exploratory and Euclidean Methods in Environmental
698 Sciences. [online] Available from: https://cran.r-project.org/web/packages/ade4/index.html
699 (Accessed 12 February 2018), 2013.

700 Clark, C. W. and Levy, D. A.: Diel Vertical Migrations by Juvenile Sockeye Salmon and the
701 Antipredation Window, Am. Nat., 131(2), 271–290, doi:10.1086/284789, 1988.

702 Coyle, K. O. and Cooney, R. T.: Water column sound scattering and hydrography around the
703 Pribilof Islands, Bering Sea, Cont. Shelf Res., 13(7), 803–827, doi:10.1016/0278-
704 4343(93)90028-V, 1993.

705 Cushing, D.: The vertical migration of planktonic Crustacea, Biol. Rev., 26(2), 158–192, 1951.

706 Davison, P. C., Koslow, J. A. and Kloser, R. J.: Acoustic biomass estimation of mesopelagic
707 fish: backscattering from individuals, populations, and communities, ICES J. Mar. Sci., 72(5),
708 1413–1424, doi:10.1093/icesjms/fsv023, 2015.

709 Dekshenieks, M., Donaghay, P., Sullivan, J., Rines, J., Osborn, T. and Twardowski, M.:
710 Temporal and spatial occurrence of thin phytoplankton layers in relation to physical processes,
711 Mar. Ecol. Prog. Ser., 223, 61–71, doi:10.3354/meps223061, 2001.

712 Demarcq, H. and Faure, V.: Coastal upwelling and associated retention indices derived from
713 satellite SST. Application to Octopus vulgaris recruitment, Oceanol. Acta, 23(4), 391–408,
714 doi:10.1016/S0399-1784(00)01113-0, 2000.

715 Diankha, O., Ba, A., Brehmer, P., Brochier, T., Sow, B. A., Thiaw, M., Gaye, A. T., Ngom, F.
716 and Demarcq, H.: Contrasted optimal environmental windows for both sardinella species in
717 Senegalese waters, Fish. Oceanogr., 27(4), 351–365, doi:10.1111/fog.12257, 2018.

718 Donaldson, H. A.: Sound scattering by marine organisms in the northeastern Pacific Ocean,
719 Oregon State Univ. [online] Available from:
720 https://ir.library.oregonstate.edu/concern/graduate_thesis_or_dissertations/cf95jd98h, 1967.

721 Emerson, S., Stump, C. and Nicholson, D.: Net biological oxygen production in the ocean:
722 Remote in situ measurements of O2 and N2 in surface waters, Glob. Biogeochem. Cycles,
723 22(3), doi:10.1029/2007GB003095, 2008.

Estrade, P., Marchesiello, P., De Verdière, A. C. and Roy, C.: Cross-shelf structure of coastal upwelling: A two — dimensional extension of Ekman's theory and a mechanism for inner shelf upwelling shut down, J. Mar. Res., 66(5), 589–616, doi:10.1357/002224008787536790, 2008.

Evans, R. A. and Hopkins, C. C. E.: Distribution and standing stock of zooplankton sound-scattering layers along the north Norwegian coast in February-March, 1978, Sarsia, 66(2), 147–160, doi:10.1080/00364827.1981.10414532, 1981.

Fässler, S. M. M., Fernandes, P. G., Semple, S. I. K. and Brierley, A. S.: Depth-dependent swimbladder compression in herring Clupea harengus observed using magnetic resonance imaging, J. Fish Biol., 74(1), 296–303, 2009.

Foote, K. G., Knudsen, H. P., Vestnes, G., MacLennan, D. N. and Simmonds, E. J.: Technical Report: '"Calibration of acoustic instruments for fish density estimation: A practical guide,"' J. Acoust. Soc. Am., 83(2), 831–832, doi:10.1121/1.396131, 1987.

Fortier, L. and Harris, R.: Optimal foraging and density-dependent competition in marine fish larvae, Mar. Ecol.-Prog. Ser., 51, 19–33, doi:10.3354/meps051019, 1989.

Gausset, M. and Turrel, W. R.: Deep sound scattering layers in the Faroe Shetland channel., Scientific Report, FRS Marine Laboratory, Aberdeen. [online] Available from: http://www.gov.scot/Uploads/Documents/IR1701.pdf (Accessed 3 June 2017), 2001.

Godø, O. R., Patel, R. and Pedersen, G.: Diel migration and swimbladder resonance of small fish: some implications for analyses of multifrequency echo data, ICES J. Mar. Sci., 66(6), 1143–1148, doi:10.1093/icesjms/fsp098, 2009.

Gómez-Gutiérrez, J., G, G.-C., Robinson, C. and V, A.-F.: Latitudinal changes of euphausiid assemblages related to dynamics of the scattering layer along Baja California, October 1994, Sci. Mar., 63, 79–91, 1999.

Gray, C.: Do Thermoclines Explain the Vertical Distributions of Larval Fishes in the Dynamic Coastal Waters of South-eastern Australia?, Mar. Freshw. Res., 47(2), 183, doi:10.1071/MF9960183, 1996.

Gray, C. A. and Kingsford, M. J.: Variability in thermocline depth and strength, and relationships with vertical distributions of fish larvae and mesozooplankton in dynamic coastal waters, Mar. Ecol. Prog. Ser., 247, 211–224, doi:10.3354/meps247211, 2003.

Haney, J. F.: Diel Patterns of Zooplankton Behavior, Bull. Mar. Sci., 43(3), 583–603, 1988.

Hidaka, K., Kawaguchi, K., Murakami, M. and Takahashi, M.: Downward transport of organic carbon by diel migratory micronekton in the western equatorial Pacific: its quantitative and qualitative importance, Deep Sea Res. Part I : Oceanogr. Res. Pap., 48(8), 1923–1939, doi:10.1016/S0967-0637(01)00003-6, 2001.

Holliday, D. V., Greenlaw, C. F. and Donaghay, P. L.: Acoustic scattering in the coastal ocean at Monterey Bay, CA, USA: Fine-scale vertical structures, Cont. Shelf Res., 30(1), 81–103, doi:10.1016/j.csr.2009.08.019, 2010.

Jacox, M. G., Edwards, C. A., Hazen, E. L. and Bograd, S. J.: Coastal Upwelling Revisited: Ekman, Bakun, and Improved Upwelling Indices for the U.S. West Coast, J. Geophys. Res. Oceans, 123(10), 7332–7350, doi:10.1029/2018JC014187, 2018.

JPL OurOcean Project: GHRSST Level 4 G1SST Global Foundation Sea Surface Temperature Analysis. Ver. 1. PO.DAAC, CA, USA, Dataset accessed [2019-05-05] at https://doi.org/10.5067/GHG1S-4FP01, 2010.

Kelley, D.: oce: Analysis of Oceanographic Data. [online] Available from: https://cran.r-project.org/web/packages/oce/ (Accessed 14 February 2018), 2015.

Kloser, R. J., Ryan, T., Sakov, P., Williams, A. and Koslow, J. A.: Species identification in deep water using multiple acoustic frequencies, Can. J. Fish. Aquat. Sci., 59(6), 1065–1077, doi:10.1139/f02-076, 2002.

Lampert, W.: The Adaptive Significance of Diel Vertical Migration of Zooplankton, Funct. Ecol., 3(1), 21–27, doi:10.2307/2389671, 1989.

Lee, H., Cho, S., Kim, W. and Kang, D.: The diel vertical migration of the sound-scattering layer in the Yellow Sea Bottom Cold Water of the southeastern Yellow sea: focus on its relationship with a temperature structure, Acta Oceanol. Sin., 32(9), 44–49, doi:10.1007/s13131-013-0351-z, 2013.

Lehodey, P., Conchon, A., Senina, I., Domokos, R., Calmettes, B., Jouanno, J., Hernandez, O. and Kloser, R.: Optimization of a micronekton model with acoustic data, ICES J. Mar. Sci., 72(5), 1399–1412, doi:10.1093/icesjms/fsu233, 2015.

Machu, E., Capet, X., Estrade, P. A., Ndoye, S., Brajard, J., Baurand, F., Auger, P.-A., Lazar, A. and Brehmer, P.: First Evidence of Anoxia and Nitrogen Loss in the Southern Canary Upwelling System, Geophys. Res. Lett., 5(46), doi:10.1029/2018GL079622, 2019.

MacLennan, D. N., Fernandes, P. G. and Dalen, J.: A consistent approach to definitions and symbols in fisheries acoustics, ICES J. Mar. Sci., 59(2), 365–369, doi:10.1006/jmsc.2001.1158, 2002.

Maechler, M., Rousseeuw, P., Struyf, A., Hubert, M. and Hornik, K.: Package 'cluster,' Version, 1(4), 6–7 [online] Available from: http://cran.r-project.org/web/packages/cluster/cluster.pdf, 2014.

Marchal, E., Gerlotto, F. and Stéquert, B.: On the relationship between scattering layer, thermal structure and tuna abundance in the eastern Atlantic equatorial current system., Oceano. Acta, 16(3), 261–272, 1993.

Mbaye, B. C., Brochier, T., Echevin, V., Lazar, A., Lévy, M., Mason, E., Gaye, A. T. and Machu, E.: Do Sardinella aurita spawning seasons match local retention patterns in the Senegalese–Mauritanian upwelling region?, Fish. Oceanogr., 24(1), 69–89, doi:10.1111/fog.12094, 2015.

Meester, L. D.: Diel Vertical Migration, in Encyclopedia of Inland Waters, edited by G. E. Likens, pp. 651–658, Academic Press, Oxford., 2009.

Ndour, I., Berraho, A., Fall, M., Ettahiri, O. and Sambe, B.: Composition, distribution and abundance of zooplankton and ichthyoplankton along the Senegal-Guinea maritime zone (West Africa), Egypt. J. Aquat. Res., 44(2), 109–124, doi:10.1016/j.ejar.2018.04.001, 2018.

Ndoye, S., Capet, X., Estrade, P., Sow, B., Dagorne, D., Lazar, A., Gaye, A. and Brehmer, P.: SST patterns and dynamics of the southern Senegal-Gambia upwelling center, J. Geophys. Res. Oceans, 119(12), 8315–8335, doi:http://dx.doi.org/10.1002/2014jc010242, 2014.

Ndoye, S., Capet, X., Estrade, P., Sow, B., Machu, E., Brochier, T., Döring, J. and Brehmer, P.: Dynamics of a "low-enrichment high-retention" upwelling center over the southern Senegal shelf, Geophys. Res. Lett., 44(10), 5034–5043, doi:10.1002/2017GL072789, 2017.

Netburn, A. N. and Koslow, J. A.: Dissolved oxygen as a constraint on daytime deep scattering layer depth in the southern California current ecosystem, Deep Sea Res. Part I: Oceanogr. Res. Pap., 104, 149–158, doi:10.1016/j.dsr.2015.06.006, 2015.

Ohman, M. D., Frost, B. W. and Cohen, E. B.: Reverse Diel Vertical Migration: An Escape from Invertebrate Predators, Science, 220(4604), 1404–1407, doi:10.1126/science.220.4604.1404, 1983.

Olla, B. and Davis, M.: Effects of physical factors on the vertical distribution of larval walleye pollock Theragra chalcogramma under controlled laboratory conditions, Mar. Ecol. Prog. Ser., 63, 105–112, doi:10.3354/meps063105, 1990.

Perrot, Y., Brehmer, P., Habasque, J., Roudaut, G., Behagle, N., Sarré, A. and Lebourges-Dhaussy, A.: Matecho: An Open-Source Tool for Processing Fisheries Acoustics Data, Acoust. Aust., 46(2), 241–248, doi:10.1007/s40857-018-0135-x, 2018.

R Core Team: R: a language and environment for statistical computing, R Foundation for Statistical Computing, Vienna, Austria. [online] Available from: https://www.R-project.org/, 2016.

Rebert, J. P.: Hydrologie et dynamique des eaux du plateau continental sénégalais, Doc. Scient, CRODT, Sénégal. [online] Available from: http://horizon.documentation.ird.fr/exl-doc/pleins_textes/divers11-12/17490.pdf (Accessed 3 June 2017), 1983.

Rojas, P. M. and Landaeta, M. F.: Fish larvae retention linked to abrupt bathymetry at Mejillones Bay (northern Chile) during coastal upwelling events, Lat. Am. J. Aquat. Res., 42(5), 989–1008, doi:10.3856/vol42-issue5-fulltext-6, 2014a.

Rojas, P. M. and Landaeta, M. F.: Fish larvae retention linked to abrupt bathymetry at Mejillones Bay (northern Chile) during coastal upwelling events, Lat. Am. J. Aquat. Res., 42(5), 989–1008, doi:10.3856/vol42-issue5-fulltext-6, 2014b.

Röpke, A.: Do larvae of mesopelagic fishes in the Arabian Sea adjust their vertical distribution to physical and biological gradients?, Mar. Ecol. Prog. Ser., 101, 223–235, doi:10.3354/meps101223, 1993.

Roy, C.: An upwelling-induced retention area off Senegal: a mechanism to link upwelling and retention processes, South Afr. J. Mar. Sci., 19(1), 89–98, doi:10.2989/025776198784126881, 1998.

839 Sánchez-Velasco, L., Jimenez Rosenberg, S. and Lavín, M.: Vertical Distribution of Fish
840 Larvae and Its Relation to Water Column Structure in the Southwestern Gulf of California1,
841 Pac. Sci., 61, 533–548, doi:10.2984/1534-6188(2007)61[533:VDOFLA]2.0.CO;2, 2007.

842 Sengupta, A., Carrara, F. and Stocker, R.: Phytoplankton can actively diversify their migration
843 strategy in response to turbulent cues, Nature, 543(7646), 555, 2017.

844 Simmonds, J. and MacLennan, D. N., Eds.: Fisheries Acoustics: Theory and Practice., in
845 Fisheries Acoustics, pp. i–xvii, Blackwell Publishing Ltd., 2005.

846 Steele, J. H., Collie, J. S., Bisagni, J. J., Gifford, D. J., Fogarty, M. J., Link, J. S., Sullivan, B.
847 K., Sieracki, M. E., Beet, A. R. and Mountain, D. G.: Balancing end-to-end budgets of the
848 Georges Bank ecosystem, Prog. Oceanogr., 74(4), 423–448, 2007.Stranne, C., Mayer, L.,
849 Jakobsson, M., Weidner, E., Jerram, K., Weber, T. C., Anderson, L. G., Nilsson, J., Björk, G.
850 and Gårdfeldt, K.: Acoustic mapping of mixed layer depth, Ocean Sci., 14(3), 503–514,
851 doi:https://doi.org/10.5194/os-14-503-2018, 2018.

852 Teisson, C.: Le phénomène d'upwelling le long des côtes du Sénégal : caractéristiques
853 physiques et modélisation, Doc. Scient, CRODT, Dakar. [online] Available from:
854 http://www.documentation.ird.fr/hor/fdi:15418 (Accessed 23 January 2018), 1983.

855 Thiaw, M., Auger, P.-A., Ngom, F., Brochier, T., Faye, S., Diankha, O. and Brehmer, P.: Effect
856 of environmental conditions on the seasonal and inter-annual variability of small pelagic fish
857 abundance off North-West Africa: The case of both Senegalese sardinella, Fish. Oceanogr.,
858 doi:10.1111/fog.12218, 2017.

859 Tiedemann, M. and Brehmer, P.: Larval fish assemblages across an upwelling front: Indication
860 for active and passive retention, Estuar. Coast. Shelf Sci., 187, 118–133,
861 doi:10.1016/j.ecss.2016.12.015, 2017.

862 Tonidandel, S. and LeBreton, J. M.: Relative Importance Analysis: A Useful Supplement to
863 Regression Analysis, J. Bus. Psychol., 26(1), 1–9, doi:10.1007/s10869-010-9204-3, 2011.

864 Torgersen, T., Kaartvedt, S., Melle, W. and Knutsen, T.: Large scale distrlbution of acoustical
865 scattering layers at the Norwegian continental shelf and the Eastern Norwegian Sea, Sarsia,
866 82(2), 87–96, 1997.

867 Touré, D.: Variation quantitative du zooplancton dans la région du Cap- Vert de septembre
868 1970 à août 1971., Doc. Scient., CRODT, Dakar, Sénégal., 1971.

869 Urmy, S. S. and Horne, J. K.: Multi-scale responses of scattering layers to environmental
870 variability in Monterey Bay, California, Deep Sea Res. Part I: Oceanogr. Res. Pap., 113, 22–
871 32, doi:10.1016/j.dsr.2016.04.004, 2016.

872 Ward, J. H.: Hierarchical Grouping to Optimize an Objective Function, J. Am. Stat. Assoc.,
873 58(301), 236–244, doi:10.1080/01621459.1963.10500845, 1963.

874 White, M. D.: Horizontal distribution of pelagic zooplankton in relation to predation gradients,
875 Ecography, 21(1), 44–62, doi:10.1111/j.1600-0587.1998.tb00393.x, 1998.

876 Wilcox, R.: Chapter 12 - ANCOVA, in Introduction to Robust Estimation and Hypothesis
877 Testing (Fourth Edition), edited by R. Wilcox, pp. 693–740, Academic Press., 2017.

878 Yasuma, H., Sawada, K., Ohshima, T., Miyashita, K. and Aoki, I.: Target strength of
879 mesopelagic lanternfishes (family Myctophidae) based on swimbladder morphology, ICES J.
880 Mar. Sci., 60(3), 584–591, doi:10.1016/S1054-3139(03)00058-4, 2003.

881 Yoon, W., Nival, P., Choe, S., Picheral, M. and Gorsky, G.: Vertical distribution and nutritional
882 behaviour of Cyclothone braueri, Nematoscelis megalops, Meganyctiphanes norvegica and
883 Salpa fusiformis in the NW Mediterranean mesopelagic zone, ICES CM F, 1–28, 2007.

11 Tables

Table 1: Result of ANCOVA models between thickness of sound scattering layers (SSLs) and environmental parameters (temperature, density, dissolved oxygen, chlorophyll-*a*, diel period and bottom depth) in the inshore area (G1) and the offshore area (G2). [G1: Multiple R-squared: 0.869, Adjusted R-squared: 0.8515, *p*-value < 0.001]; and [G2: Multiple R-squared: 0.8557, Adjusted R-squared: 0.7956, *p*-value < 0.001]. Significant *p*-value in bold.

Variable	Significance		Explained deviance (%)		Total explained variance (%)	
	Inshore (G1)	Offshore (G2)	Inshore (G1)	Offshore (G2)	Inshore (G1)	Offshore (G2)
Bottom depth	**0.001**	**0.005**	55.86	28.05	86.9	85.57
Diel period (Night)	**0.007**	**0.008**	31.02	28.33		
Temperature		**0.007**		11.29		
Density		**0.008**		10.35		
Oxygen		**0.007**		7.53		

Table 2: Result of ANCOVA models between depth of sound scattering layers (SSLs) and environmental parameters (temperature, density, dissolved oxygen, chlorophyll-*a*, diel period, and bottom depth) in the inshore area (G1) and the offshore area (G2). [G1: Multiple R-squared: 0.8056, Adjusted R-squared: 0.7797, *p*-value: 0.001]; and [G2: Multiple R-squared: 0.8557, Adjusted R-squared: 0.7956, *p*-value: 0,000]. Significant *p*-value in bold.

Variable	Significance		Explained deviance (%)		Total explained variance (%)	
	Inshore (G1)	Offshore (G2)	Inshore (G1)	Offshore (G2)	Inshore (G1)	Offshore (G2)
Bottom depth	**0.001**	**0.005**	55.86	28.05	80.56	85.57
Diel period (Night)	**0.021**	**0.008**	31.02	28.33		
Temperature		**0.007**		11.29		
Density		**0.008**		10.35		
Oxygen		**0.007**		7.53		

Table 3: Result of ANCOVA models between sound scattering layers (SSLs) density ($\log(s_A)$) and environmental parameters (temperature, density, dissolved oxygen, chlorophyll-*a*, diel period, and bottom depth) in the inshore area (G1) and the offshore area (G2). [G1: Multiple R-squared: 0.398, Adjusted R-squared: 0.3178, *p*-value: 0.022]; and [G2: Multiple R-squared: 0.3448, Adjusted R-squared: -0.01258, *p*-value: 0.490]. Significant *p*-value in bold.

Variable	Significance		Explained deviance (%)		Total explained variance (%)	
	Inshore (G1)	Offshore (G2)	Inshore (G1)	Offshore (G2)	Inshore (G1)	Offshore (G2)
Bottom depth	**0.008**	0.357	33.06	7.56	39.8	34.48
Temperature	0.119	0.273	6.73	5.17		
Diel period (Night)		0.007	0.546	7.22		
Density		0.008	0.250	5.56		
Oxygen		0.007	0.166	5.19		

12 Figures

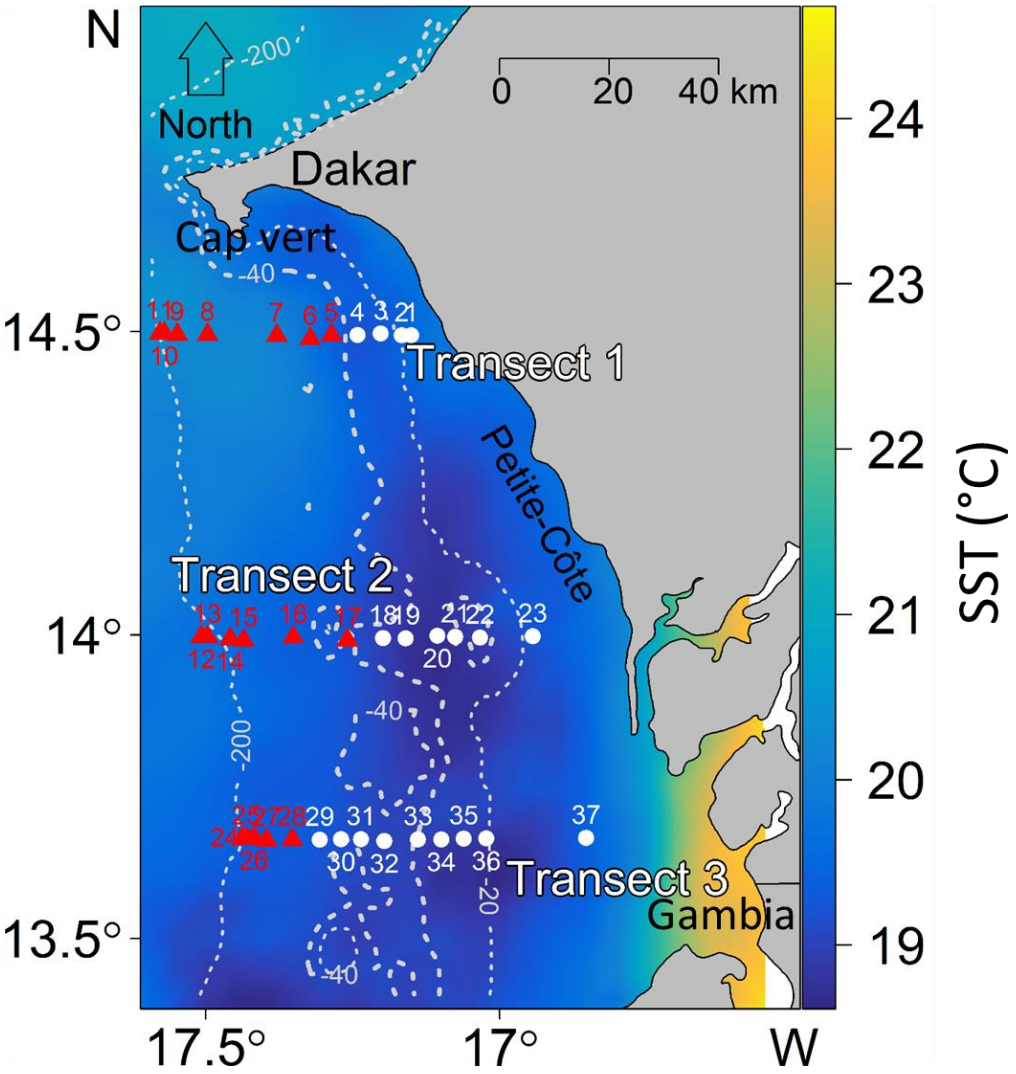

Fig. 1: Location of the survey area off the southern Senegalese (West African) coast. The hydroacoustic survey was conducted with FRV Antea (IRD) from Dakar (Cap Vert peninsula) to the northern border of Gambia. CTD-probes collected data at stations along three transects perpendicular to the coast (T1 to T3). Sea surface temperature (SST, °C) were averaged over the three days of CTD sampling from the 6–8 March 2013. Stations of Group 1 (white circles) occurred in the inshore zone, whereas stations of Group 2 (red triangles) were situated more offshore. The dashed white lines represent bathymetry (in m).

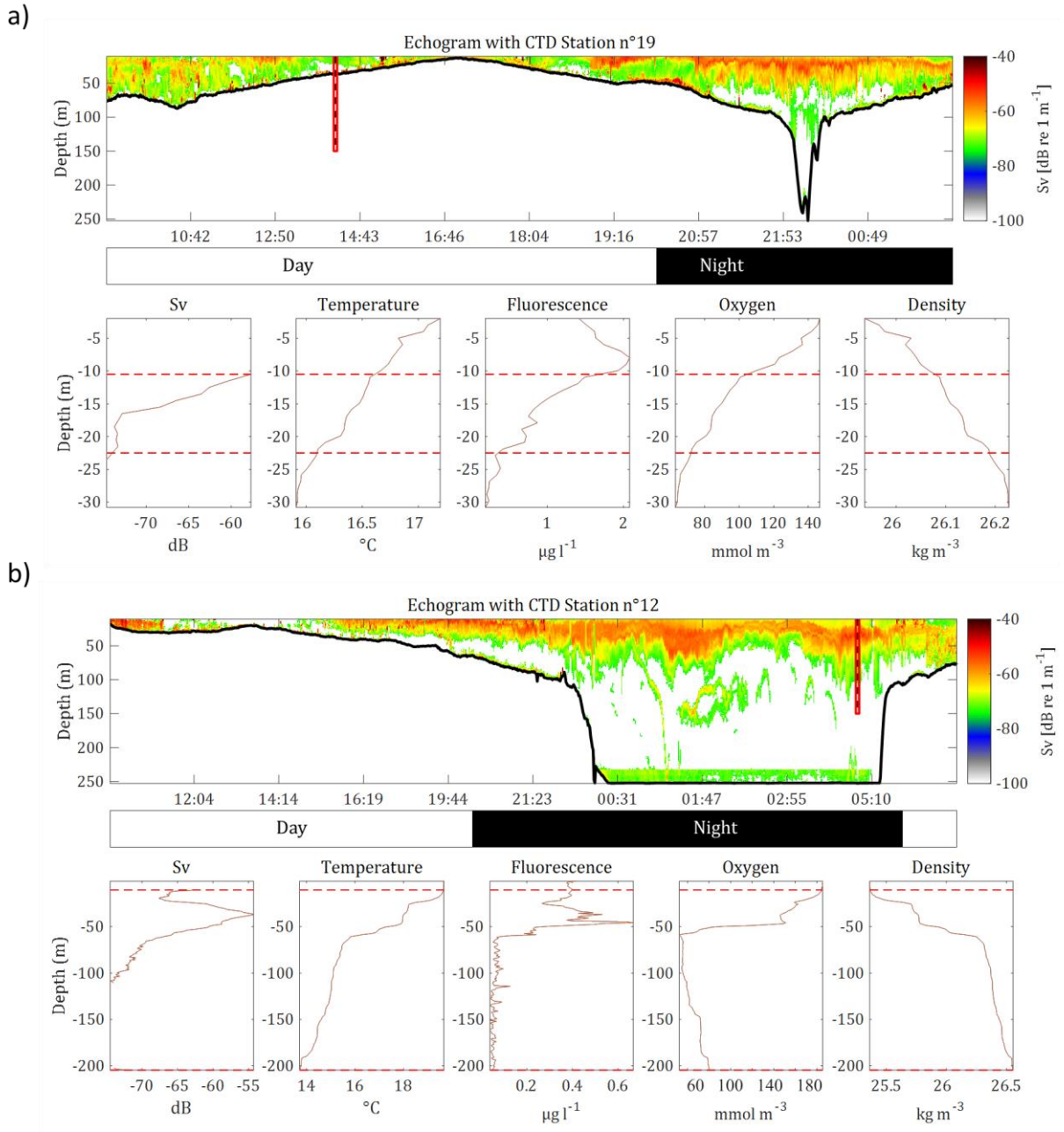

Fig. 2: Echograms and associated vertical acoustic profiles as well as physico-chemical parameters (CTD data) for two example stations: (a) station 19 in the “inshore area” and (b) station 12 in the “offshore area”. For both (a) and (b), top panels are echogram data collected along the transect, *i.e.,* 1000 ESU (elementary sampling unit) of 0.1 nmi, whereas the bottom panels depict acoustic and environmental data (depicted by the red vertical line in top panels). Environmental data for the sound scattering layer (SSL) collected at the stations at the location depicted by dotted

vertical lines. Data represent mean conditions for the station collected within an area of 0.1 nmi area around the station: acoustic volume backscattering strength (S_v) SSL, temperature profile SSL, CHL profile SSL, oxygen profile SSL, and density profile SSL. The horizontal dashed lines in all profiles represent the SSL thickness i.e. the upper and lower SSLs limit.

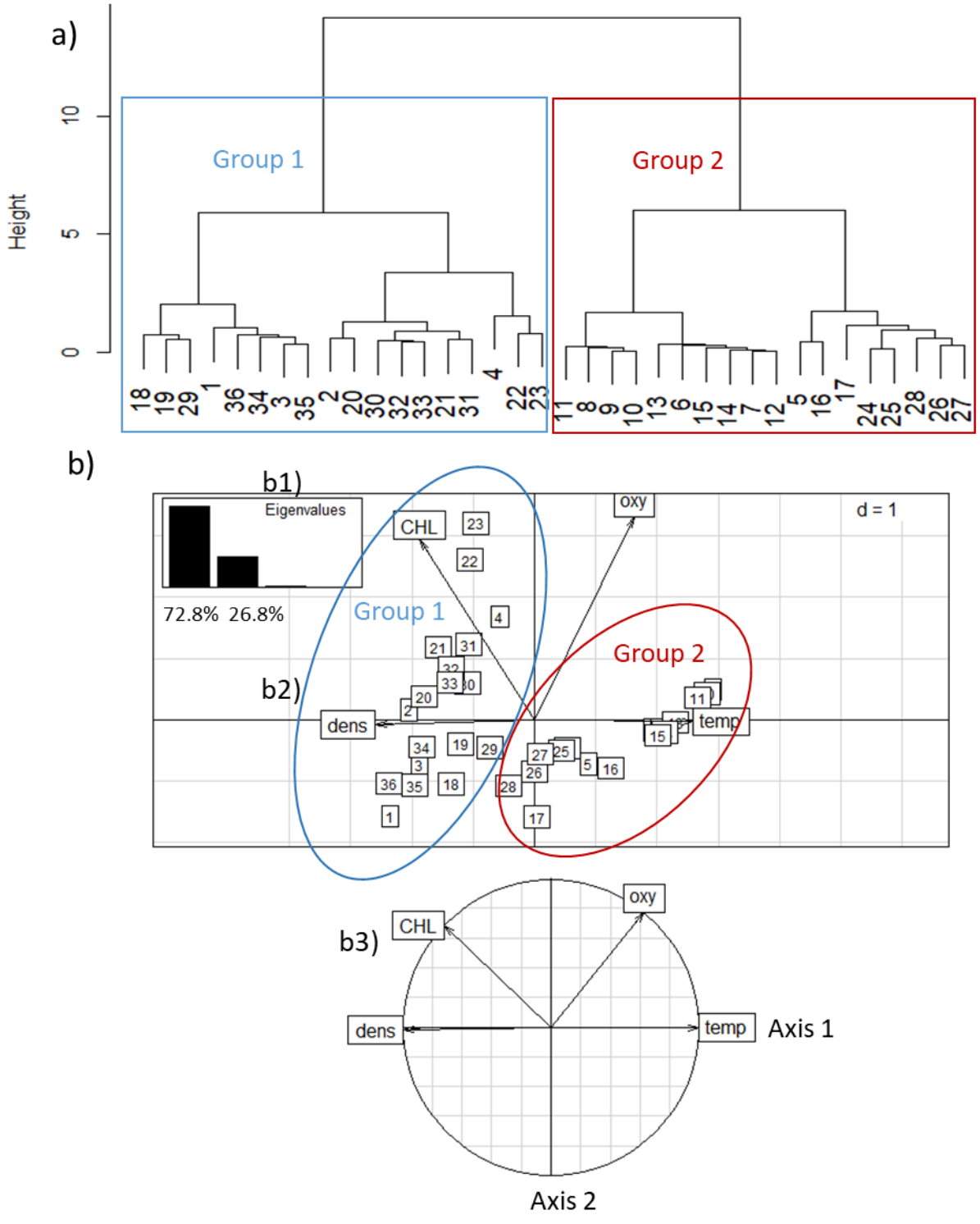

Fig. 3: Discrimination of 36 CTD stations off the Senegalese coast: (1) Two groups of stations were discriminated based on temperature (temp), chlorophyll-*a* (CHL), dissolved oxygen (oxy), and density (dens). (2) Principal Components Analysis of environmental parameters for all 36 stations. (a) Eigenvalue diagram; (b) Factor plane;

(c) Correlation circle. Group 1 are stations located in the inshore area (n = 18), Group 2 are stations located in the offshore area (n = 18).

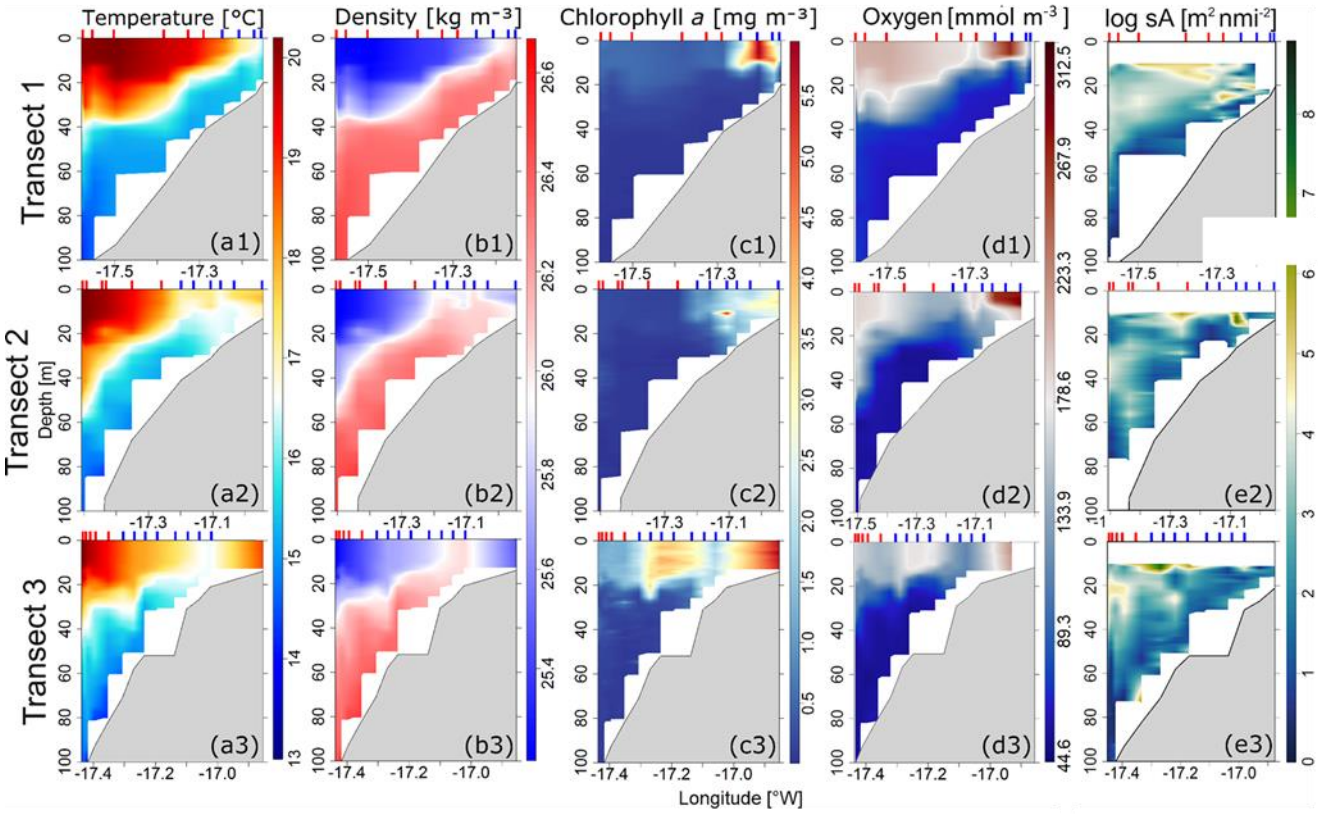

Fig. 4: Mean vertical profiles of (a) temperature, (b) density, (c) chlorophyll-a concentration, (d) dissolved oxygen, and (e) square rooted Nautical Area Scattering Coefficient (s_A) in the three transects (T1, T2, T3; see Fig. 1) with positions of vertical probe stations CTD in the inshore area (vertical line in blue (G1)) and the offshore area (vertical line in red (G2)).

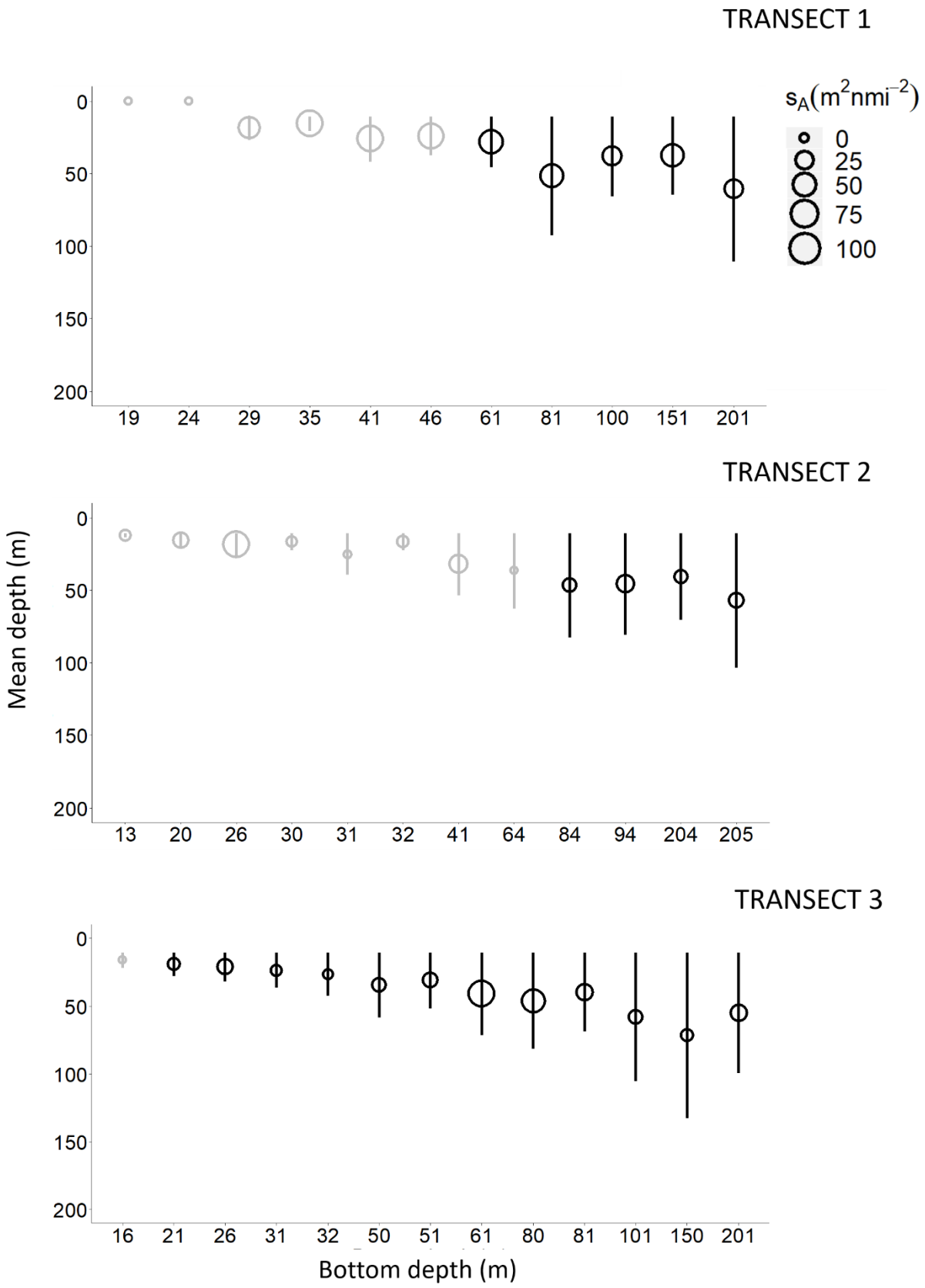
TRANSECT 1
$s_A(m^2nmi^{-2})$
0
25
50
75
100
0
50
100
150
200
19
24
29
35
41
46
61
81
100
151
201
TRANSECT 2
Mean depth (m)
0
50
100
150
200
13
20
26
30
31
32
41
64
84
94
204
205
TRANSECT 3
0
50
100
150
200
16
21
26
31
32
50
51
61
80
81
101
150
201
Bottom depth (m)

9

10

Fig. 5: Sound scattering layers (SSLs) mean depth (empty circle) according to their bottom depth, with their associated thickness (line, in meter), and SSL mean Nautical Area Scattering Coefficient (NASC or s_A in m^2 nmi^{-2}), along transect 1 (south), 2 (intermediary), and 3 (north) during nighttime (black) and daytime (grey) sampling periods.

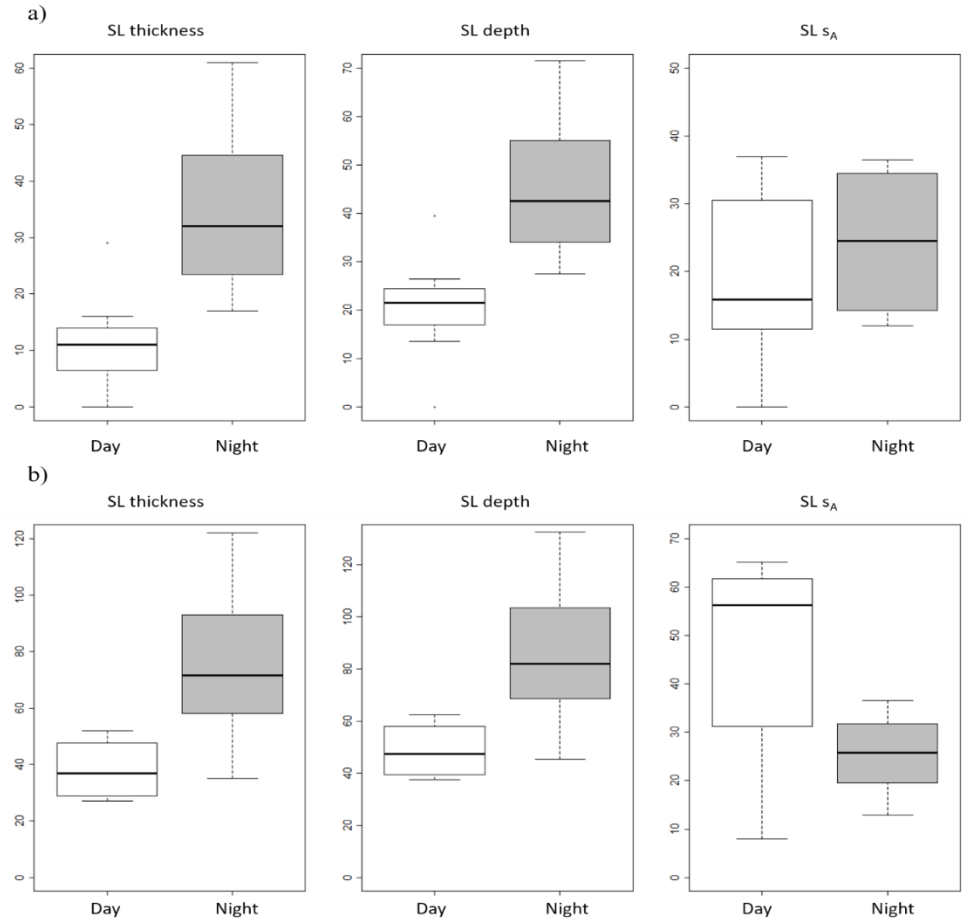

Fig. 6: Box plot (minimum, maximum, and median) of sound scattering layers (SSLs) mean depth (m), thickness (m), and relative biomass (s_A in m^2 nmi^{-2}) grouped by diel period (days/night) for (a) inshore area; and (b) offshore area over the Senegalese continental shelf.